ROBUST CAMERA MOTION ESTIMATION IN VIDEO SEQUENCES

Xiaobo An, Xueying Qin, Guofeng Zhang,Wei Chen, Hujun Bao
State Key Lab of CAD & CG, Zhejiang University
China, 310058

Keywords: Motion Estimation.

Abstract: Camera motion estimation of video sequences requires robust recovery of camera parameters and is a cumbersome task concerning arbitrarily complex scenes in video sequences. In this paper, we present a novel algorithm for robust and accurate estimation of camera motion. We insert a virtual frame between each pair of consecutive frames, through which the in-between camera motion is decomposed into two separate components, i.e., pure rotation and pure translation. Given matched feature points between two frames, one point set corresponding to the far scene is chosen, which is used to estimate initial camera motion. We further refine it recursively by a non-linear optimizer, yielding the final camera motion parameters. Our approach achieves accurate estimation of camera motion and avoids instability of camera tracking. We demonstrate high stability, accuracy and performance of our algorithm with a set of augmented reality applications based on acquired video sequences.

1 INTRODUCTION

Structure and motion problem is one of the most important research topics in the past decade. Generally speaking, there are two steps to fulfill this task. Feature tracking (Zivkovic and van der Heijden, 2002; Georgescu and Meer, 2004) is first performed to find the correspondences between two images. Based on the correspondences, camera tracking and/or structure reconstruction can be accomplished by applying two-view (epipolar geometry) (Zhang, 1998; Zhang and Loop, 2001) or multi-view (trilinear tensor) (Shashua and Werman, 1995; Stein and Shashua, 2000; Sharp et al., 2004; Hartley and Zisserman, 2000) based techniques. Many methods aim to estimate structure and motion by using special constraints, like lines, features on planes, *etc*. (Johansson, 1990; Alon and Sclaroff, 2000; Pollefeys et al., 2004). These constraints are typically too strong to be applied in general scenes. Kalman filter based methods (Azarbayejani and Pentland, 1995) can be used either for the estimation of initial solution or for bundle adjustment involved in the camera motion estimation. However, the linear update introduced by Kalman filter is not optimal for highly non-linear structure and motion problem.

Structure and motion estimation algorithms are known to be far away from perfect. First, the accuracy of traditional feature tracking methods usually does not meet the practical requirements, because they may fail to produce correct matches ascribing to inter-occlusions, intersections, moving objects, large motions or ambiguities. Although some outlier rejection techniques (Zhang, 1998) are introduced to address this problem, they never promise to pick out all outliers. Second, the effects caused by the camera rotation and translation may interfere with each other. When the number of unknown parameters increases, the stability tends to drop dramatically (MacLean, 1999), especially when the epipolar geometry is ill-posed due to small camera motion. Third, the widely used non-linear optimization techniques often get stuck in local minima (Kahl and Heyden, 2001). Small camera motion and noisy feature correspondences aggravate this problem. Therefore, the choice of the initial value for an optimizer is very crucial.

For outdoor scenes taken by a hand-held video camera, robust camera motion estimation is of great importance. One typical example is Augmented Reality (AR) that has been widely used in many applications such as environmental assessments (Qin et al.,

An X., Qin X., Zhang G., Chen W. and Bao H. (2006).
ROBUST CAMERA MOTION ESTIMATION IN VIDEO SEQUENCES.
In *Proceedings of the First International Conference on Computer Vision Theory and Applications*, pages 294-302
DOI: 10.5220/0001361702940302

2002) and archeology (Cornelis et al., 2001; Pollefeys et al., 2004). When virtual objects are located on the background scenes, an observer is very sensitive to the accuracy of camera parameters and hence accurate estimation of camera motion is very crucial in AR-based applications.

The contributions of this paper improve upon previous approaches in several aspects. First, our approach does not impose any constraints on scenes. This makes our approach inherently suitable for general scenes. Second, our approach eliminates the high correlation between the camera rotation and translation by treating them separately. And the estimation process involves five parameters of unknowns without any redundancy. In addition, correct estimation of camera translation direction can be easily achieved, which is regarded as a key but intractable problem in camera motion estimation. In consequence, no special optimizer is needed for computing precise parameters of camera motion.

The remainder of this paper is organized as follows. After a brief introduction on related work in Section 2, a conceptual overview is given in Section 3. In Section 4 we present the proposed algorithm for two consecutive frames. Optimization over continuous frames of a video sequence is introduced in Section 5. Experiments results and discussions are described in Section 6. Finally, we conclude the whole paper in Section 7.

2 BASIC STRUCTURE OF A SCRIPT

Many efforts have been put on robust camera motion estimation. Traditional methods try to recover the camera motion by calculating the fundamental matrix or the essential matrix, which usually includes seven degrees of freedom. Whereas, camera motion has actually five degrees of freedom. Researchers have focused on the robust determination of epipolar geometry (Zhang, 1998; Zhang and Loop, 2001) by minimizing the epipolar errors. The epipolar errors of correspondences can be made much less than one pixel (Zhang and Loop, 2001). However, this does not lead to a small 3D projection error and accurate camera motion (Chen et al., 2003). Wang and Tsui (Wang and Tsui, 2000) report that the resultant rotation matrix and translation vector could be quite unstable.

Structure from motion focuses on the recovery of 3D models contained in the scenes. Pollefeys *et al.* (Pollefeys et al., 2004) propose an elegant approach to recover structure and motion simultaneously. Two key frames which exhibit obvious motion are chosen to compute camera motion, and initial 3D models of the targets are constructed. Subsequently, relative camera motion at any frame between these two key frames is obtained. Additional refinements on both structure and motion are performed for each frame. This method is hard to deal with general scenes because it makes use of the affine-model based on two assumptions, i.e., frames can be divided into multiple subregions in which all points are coplanar and these subregions do not change orders in the video sequence. Obviously, these assumptions no longer hold for scenes containing inter-occlusions and intersections objects.

Some researchers try to calculate the camera translation separately (Jepson and Heeger, 1991; MacLean, 1999). One technique named ”subspace methods” generates constraints perpendicular to the translation vector of camera motion, and is feasible for the recovery of the translation vector. Recently, Nist$\acute{e}$r *et al.* (Nistér, 2004) points out that the epipolar based method exploiting seven or eight pairs of matched points may result in inaccurate camera parameters. They instead propose to compute the essential matrix with only five pairs of point correspondences, achieving minimal redundancy. With the computed essential matrix, the camera motion can be estimated using SVD algorithm. This indirect approach is different from ours, which evaluates camera motion directly.

Typically, an efficient optimization process is required to achieve more stable results over the video sequence. This kind of refinement is often referred as bundle adjustment technique (Wong and Chang, 2004). It is shown that the bundle adjustment technique can also be applied to drift removal (Cornelis et al., 2004).

3 VARIABLES

For each video sequence, we assume that the intrinsic parameters of the camera are unchanged and have been calibrated in advance. The study on camera motion estimation can be concentrated on the computation of extrinsic camera parameters in each frame, which is composed of one rotation matrix R and one translation vector T.

As an overview, we first introduce the camera model briefly in conventional notations. We denote a 3D point and its projective depth by homogenous coordinates $\mathbf{X} = (X, Y, Z, 1)^\top$ and λ. The homogenous coordinates $\mathbf{u} = (x, y, 1)^\top$ specify its projection in a 2D image. The 3×3 rotation matrix and triple translation vector are defined as $R = \{r_k, k = 0, ..., 8\}$ and $T = (t_0, t_1, t_2)^\top$, respectively. Throughout this paper we will use the subscript i to denote the frame number, the subscript j to specify the index number of feature points, E for the essential matrix, and I for the identity matrix.

For a video sequence containing N frames, we define the first frame as the reference frame. The camera model is built upon the camera coordinate system corresponding to the reference frame. Suppose that the number of 3D points is M, and the camera motion from the first frame to the ith frame is denoted by $\mathbf{P}_i$ with $\mathbf{P}_0 = (I|0)$, R_i and T_i are the rotation matrix and translation vector from frame i to frame $i+1$, it yields:

$$\begin{gathered}\lambda_1\mathbf{u}_{1,j} = \mathbf{P}_0\mathbf{X}_j, \quad \lambda_i\mathbf{u}_{i,j} = \mathbf{P}_i\mathbf{X}_j, \\ \lambda_{i+1}\mathbf{u}_{i+1,j} = (R_i|T_i)\mathbf{P}_i\mathbf{X}_j = \mathbf{P}_{i+1}\mathbf{X}_j \\ i = 1, ..., N, \;\; j = 1, ..., M\end{gathered} \tag{1}$$

Our goal is to recover all R_i and T_i, $i = 1, ..., N-1$. Note that, 3D points $\mathbf{X}_j, j = 1, ..., M$ are unknown variables, while each $\mathbf{u}_{i,j}$ can be computed by any efficient feature tracking algorithm.

Given arbitrary two consecutive frames f_i and f_{i+1}, to simplify the notations, we omit the superscripts for all parameters involved in the previous frame f_i and use the superscript $'$ for those of f_{i+1}. Hence, for any 3D point $\mathbf{X}$, we have:

$$\lambda\mathbf{u} = \mathbf{P}_0\mathbf{X}, \quad \lambda'\mathbf{u}' = (R|T)\mathbf{X} = R\mathbf{X} + T \tag{2}$$

We propose to decompose the camera motion between f_i and f_{i+1} to pure rotation and pure translation by inserting a virtual frame f_v, i.e. $f_i \underset{R}{\rightarrow} f_v \underset{T}{\rightarrow} f_{i+1}$, through which R and T can be computed separately, as shown in Figure 1.

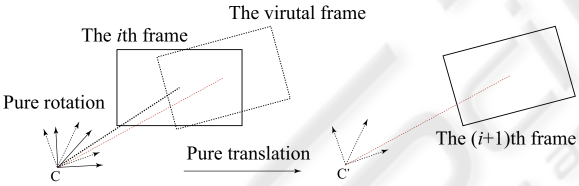

Figure 1: A virtual frame is inserted between f_i and f_{i+1}, based on which the camera motion is decomposed into pure rotation and translation.

Using the superscript $''$ to specify the parameters relating to f_v, it yields:

$$\lambda''\mathbf{u}'' = R\mathbf{X}, \;\; \lambda'\mathbf{u}' = R\mathbf{X} + T = \lambda''\mathbf{u}'' + T \tag{3}$$

Note that, the camera motion between f_i and f_{i+1} results in 2D movement $d\mathbf{u} = \mathbf{u}' - \mathbf{u}$ for each point $\mathbf{u}$ in f_i. Similar to the decomposition of the camera motion, $d\mathbf{u}$ can be viewed as the sum of two parts, namely, $d\mathbf{u}_r = \mathbf{u}'' - \mathbf{u}$, which is the 2D movement caused by pure rotation, and $d\mathbf{u}_t = \mathbf{u}' - \mathbf{u}''$, which is the 2D movement due to pure translation, hence:

$$d\mathbf{u} = (\mathbf{u}'' - \mathbf{u}) + (\mathbf{u}' - \mathbf{u}'') = d\mathbf{u}_r + d\mathbf{u}_t \tag{4}$$

Based on this decomposition, we will show how the camera motion can be recovered precisely in the next section.

4 CAMERA MOTION ESTIMATION BETWEEN TWO CONSECUTIVE FRAMES

Traditional methods usually involve redundant parameters and invoke the uncertainty of camera motion recovery. In contrast, our algorithm estimates the camera motion defined by five unknown parameters of R and T directly without redundant parameters. In addition, we intends to decompose the 2D movement of each feature point into two parts and estimate them individually. Consequently, aforementioned correlation between R and T during the computation process is avoided.

4.1 Movements of the Feature Points

We first analyze the characteristics of the 2D movements of feature points. From Equation (2), we have:

$$d\mathbf{u} = \begin{pmatrix} x' - x \\ y' - y \end{pmatrix} = \begin{pmatrix} \frac{r_0x + r_1y + r_2 + t_0/Z}{r_6x + r_7y + r_8 + t_2/Z} - x \\ \frac{r_3x + r_4y + r_5 + t_1/Z}{r_6x + r_7y + r_8 + t_2/Z} - y \end{pmatrix} \tag{5}$$

There are two extreme cases in the context of camera motion. One is pure rotation, wherein the movement of $\mathbf{u}$ is associated with three Euler angles and its 2D homogenous coordinates, while is irrelevant to the depth of corresponding 3D point. In practice, when the translation of a camera is very small compared to the depth of a 3D point, i.e., $\|T/Z\| \ll 1$, the 2D movement of this point approximates to a pure rotation. The other case is pure translation, or say:

$$\lambda'\mathbf{u}' = (I|0)\mathbf{X} + T = \lambda\mathbf{u} + \begin{pmatrix} t_0 \\ t_1 \\ t_2 \end{pmatrix} \tag{6}$$

Thus, we have:

$$d\mathbf{u} = \begin{pmatrix} x' - x \\ y' - y \end{pmatrix} = \frac{1}{\lambda'}\begin{pmatrix} t_0 \\ t_1 \end{pmatrix} - \frac{t_2}{\lambda'}\begin{pmatrix} x \\ y \end{pmatrix} \tag{7}$$

From Equation (7), it is clear that the 2D movement $d\mathbf{u}$ is depending on the projective depth λ'.

Since the translation between two consecutive frames is very small, the 2D movements of near feature points are more sensitive to the camera translation than those of far feature points. Enlightened by this observation, we seek to first compute a set of far feature points corresponding to the far region and utilize them for stable estimation of R. The far region can be viewed as a far depth layer.

4.2 Detection of the Far Depth Layers

The automatic detection of the far depth layer is performed for the first frame. In case that it fails, we can select the far feature points manually for the first frame. The automatic detection method for the first frame classifies all feature point pairs by considering their disparities. The set of points with the length of disparities larger than some given threshold is called the max-group. Likewise, the min-group refers to the set of points with the length of disparities smaller than another selected threshold. Typically, there are two circumstances, i.e., either the min-group or the max-group corresponds to the far depth layer. We compute the likeness for each circumstance and choose the one with the larger likeness. Its corresponding region is regarded as the far depth layer. In our experiments, this approach produces correct results for all outdoor scenes.

Note that, the depth layers in a video sequence may be different from view to view. For example, a far point in one frame may switch to a near point in another frame. In addition, many feature points may disappear along the video sequence. Thus, it is necessary to detect the far depth layer for each frame. For each successive frame, the automatic update of the far depth layer is performed after the estimation of the underlying camera motion, as described in Section 4.3 and 4.4. With the recovered camera parameters, we calculate corresponding 3D point for each feature point pair. We then re-select far points based on the depth of feature points, yielding the far depth layer of current frame.

4.3 Initial Estimation of the Camera Motion

It is critical to provide good initial estimations that are close to the ground-truth, because optimization processes usually lead to locally optimal solutions. Our solution is based on the assumption that the 2D movements of the far points in frames are caused almost by camera rotation. The reason is that the influence induced by the camera translation of the far points is too small to be counted at the beginning. We adopt the fixed camera model (Qin et al., 2002) to calculate the initial R based on the far depth layer. It works well between two consecutive frames, where the camera rotations are quite small.

By subtracting the movement caused by camera rotation, i.e., $d\mathbf{u}_t = d\mathbf{u} - d\mathbf{u}_r$, an initial estimation of the 2D movement due to the camera translation can be obtained. We then recover the camera translation with these 2D movements. More concretely, in order to obtain precise translation vector, we take into account two cases of the camera translation. If $t_2 = 0$, we have:

$$d\mathbf{u}_t = \begin{pmatrix} x' - x'' \\ y' - y'' \end{pmatrix} = \frac{1}{\lambda'} \begin{pmatrix} t_0 \\ t_1 \end{pmatrix} \tag{8}$$

Equation (8) means that the resultant movement is completely determined by the projective depth. Here, all 2D movement vectors take the same direction and different sizes. On the other side, the resultant movement is determined by both projective depth and its 2D location (x, y) if t_2 is nonzero.

In practice, if there is no movement along z, we set the translation vector as $T = (t_0, t_1, 0)$, and $T = (t_0, t_1, 1)$ contrariwise. Under pure translation, we have $E = [T]_\times$. Suppose that $l^{'} = E\mathbf{u} = (l_1^{'}, l_2^{'}, l_3^{'})^\top$ and $l = E^\top \mathbf{u} = (l_1, l_2, l_3)^\top$, we can calculate an initial translation T by minimizing Equation (9) using LMeds method (Zhang, 1998; Chen et al., 2003):

$$\min_T \sum_j \left(\frac{1}{\sqrt{l_1^2 + l_2^2}} + \frac{1}{\sqrt{l_1'^2 + l_2'^2}} \right) \left| \mathbf{u}^{'\top} [T]_\times \mathbf{u} \right| \tag{9}$$

The recovered R and T are rough estimated values because the movements of the far points are not caused entirely by a pure rotation. Therefore, both of $d\mathbf{u}_t$ and $d\mathbf{u}_r$ are inaccurate. To refine these results, an additional iterative optimization is required. Nevertheless, it is worthy mentioning that R and T are good enough as the initial values for the optimization. The reason for this is that the camera translation between two consecutive frames is small enough compared to the depth of the far points. Moreover, the camera translation direction is of great importance in the optimizing process. Fortunately, the 2D movements of the feature points in frames are well suitable for the estimation of the direction of T, as demonstrated by our experiments.

4.4 Iterative Estimation of Camera Motion

In this section, we use the superscript number to count the iteration step. We call the handled two frames as the previous and successive frames. By means of the initial estimations of R and T, i.e., $R^{(0)}$ and $T^{(0)}$, the 3D coordinates $\mathbf{X}_j^{(0)}$ $j = 1, ..., M$ of all feature points are recovered. For the sake of simplicity, we explain our algorithm by taking the kth iteration as our example. We assume that $R^{(k)}$, $T^{(k)}$ and $\mathbf{X_j^{(k)}}$ are known. We employ a two-step iterative method to optimize the initial estimations of R and T.

In the first step, we calculate $d\mathbf{u}_{t,j}^{(k+1)}$ for all j based on $T^{(k)}$ and $\mathbf{X}_j^{(k)}$ because the camera motion between the virtual frame and the successive frame is pure translation. Subsequently, we subtract the movement caused by translation, yielding more precise $d\mathbf{u}_{r,j}^{(k+1)}$, i.e., $d\mathbf{u}_{r,j}^{(k+1)} = d\mathbf{u}_j - d\mathbf{u}_{t,j}^{(k+1)}$. Finally, we compute $R^{(k+1)}$ by minimizing the re-projected difference D_r:

$$D_r = \sum_{j=0}^{M} (\|\mathbf{u}_j'' - \tilde{\mathbf{u}}_j''\|^2 + \|\mathbf{u}_j - \tilde{\mathbf{u}}_j\|^2), \tag{10}$$

where $\tilde{\mathbf{u}}_j$ and $\tilde{\mathbf{u}}''_j$ denote the re-projected points in the previous frame and the inserted virtual frame.

We begin the second step by fixing $R^{(k+1)}$. We re-calculate the 2D movement of all feature points caused by the camera rotation, i.e., $d\mathbf{u}_{r,j}^{(k+1)}$. The 2D movements caused by the camera translation are updated correspondingly by $d\mathbf{u}_{t,j}^{(k+1)} = d\mathbf{u}_j - d\mathbf{u}_{r,j}^{(k+1)}$. Then, we compute $T^{(k+1)}$ by minimizing the re-projected error D_t:

$$D_t = \sum_{j=0}^{M} (\|\mathbf{u}'_j - \tilde{\mathbf{u}}'_j\|^2 + \|\mathbf{u}''_j - \tilde{\mathbf{u}}''_j\|^2), \qquad (11)$$

where $\tilde{\mathbf{u}}'_j$ denotes the re-projected point in the successive frame. With $R^{(k+1)}$ and $T^{(k+1)}$, $\mathbf{X}_j^{(k+1)}$ can be achieved conveniently.

We perform this two-step optimization recursively till the sum of two errors are below some user-determined threshold ϵ:

$$D_t + D_r < \epsilon \qquad (12)$$

The nonlinear optimization is accomplished by Levenberg-Marquardt algorithm. Note that, we pick out outliers again based on projection error and the recovered 3D points after each iteration. On advantage pf our method is that only two or three unknowns are evaluated in each step. The iterative optimization minimizes the projection errors corresponding to R and T recursively. This scheme effectively eliminates the correlation of R and T, and favors robust camera motion estimation.

5 SPECIAL CONSIDERATIONS OVER VIDEO SEQUENCE

To achieve robust camera motion estimation over a video sequence, there are additional cares to be taken even if all camera motions between consecutive frames are recovered.

Structure and motion can only be approximated up to an undetermined similarity, that is, the reconstruction is subject to arbitrary scaling. Exploiting the fact that the distance of any two 3D points in the scene should be fixed, we normalize the translation vector to obtain a uniform space. More concretely, for each pair of consecutive frames, we can obtain the 3D coordinates of all feature points based on recovered camera motion, we then compute the distance between any two 3D points, and optimize a scale which keeps every distance in the successive frame constant.

On the other hand, bundle adjustment can be carried out to smooth some occasional failed camera estimation. We first use the recovered camera parameters between two consecutive frames to evaluate overall camera parameters along the video sequence and optimize the overall camera motion by Levenberg-Marquardt algorithm. We then reconstruct the scene and get a uniform depth map for the whole sequence. Next, we use the method similar to that of Pollefeys *etc.* (Pollefeys et al., 2004) to refine the in-between camera parameters between the first and the last frames. Our experiments show that bundle adjustment is very efficient for normalizing the 3D space of scenes, smoothing camera motion and removing drift over the sequence.

6 EXPERIMENTAL RESULTS AND DISCUSSIONS

We have performed several experiments on both synthetic data sets and real video sequences to examine the accuracy of our algorithm.

6.1 Synthetic Video Sequences

We first evaluate the performance based on a synthetic video sequence. We predefine the camera motion for the entire sequence and choose 300 image points for the first frame. The correspondence points through the sequence are calculated from the known camera motion and their 3D coordinates. Gaussian noise is added to both x and y image coordinates for all correspondences.

In Table 1, the ground-truth and estimated camera parameters corresponding to R and T by different methods are compared. The matching errors of feature points are simulated by a Gaussian noise whose average is 1.0 pixel. The second and third items list the results using our method, with and without iteration process (Section 4.4) respectively. It is obvious that the iterative optimization improves the accuracy much. The results by means of the Singular Value Decomposition (SVD) of the essential matrix (Wang and Tsui, 2000) are listed in the fourth item. Surprisingly, our method outperforms the SVD method even when no iteration optimization is performed.

Table 2 lists the results of our method under different Gaussian noise sizes. Here, R is represented by three Euler angles α, β and γ, and p_α, p_β and p_γ denote the percentage of differences between the recovered Euler Angles and real ones. The accuracy of T is measured by the angle difference θ_T in degrees between the recovered one and the real one. Row 2-5 show the accuracy of the camera parameters by means of our method. The numbers listed in Row 6-9 demonstrate the results by Levenberg-Marquardt op-

Table 1: Accuracy comparisons of R and T for a synthetic video sequence.

Real R			Real T
0.9999	0.0157	4e-005	9.9752
-0.0157	0.9999	0.0071	-0.5898
7e-005	-0.0071	1.0000	0.4910
R with iteration			T with iteration
0.9999	0.0151	3e-005	9.9480
-0.0151	0.9999	0.0073	-0.9022
7e-005	-0.0073	1.0000	0.5621
R without iteration			T without iteration
0.9998	0.0179	4e-005	9.9967
-0.0179	0.9998	0.0074	0.3500
8e-005	-0.0074	1.0000	0.1800
R using SVD			T using SVD
1.0000	0.0100	4e-005	1.0291
-0.0100	0.9999	0.0057	0.9212
8e-006	-0.0057	1.0000	9.9089

Table 2: Accuracy of camera motion under five noise sizes. Row 2-5 demonstrate the results using our method. The results shown in Row 6-9 are achieved by Levenberg-Marquardt optimizer directly after the initial estimation.

Noise	0.1	0.5	1.0	1.5	2.0
p_α	0.019%	0.080%	0.095%	1.005%	2.800%
p_β	0.017%	0.025%	0.055%	0.750%	2.200%
p_γ	0.002%	0.010%	0.055%	0.095%	0.300%
θ_T	0.7	1.9	3.2	6.7	14.1
p_α	0.045%	0.110%	0.175%	1.520%	3.000%
p_β	0.025%	0.055%	0.130%	1.260%	2.900%
p_γ	0.005%	0.020%	0.150%	0.180%	0.400%
θ_T	3.2	4.6	6.1	13.2	19.0

timizer after the initial estimation of camera motion. Our method produces more reasonable results.

There are two criteria to measure calibration errors. One is the distance from the matched points to their epipolar lines, called the average epipolar error. The other one is the average distance between the re-projected 2D points and the measured 2D points, called average projection error. We compare both errors among our method and traditional algorithms as shown in Figure 2. In Figure 2(a), the average epipolar error using epipolar based method (Zhang and Loop, 2001) is slightly smaller than that of our method. Figure 2(b) demonstrates that our method is superior to other approaches in the context of the projection errors. This is because small 2D residual errors do not correspond to accurate camera parameters as reported in (Chen et al., 2003). In this context, camera motion estimation methods resulting in smallest epipolar error are probably not the best choice. Instead, the projection error is a better measurement.

6.2 Real Video Sequences

We examine our algorithm on four real video sequences containing large natural scenes by integrating a virtual 3D sculpture model into each video sequence. The intrinsic parameters are calibrated with OpenCV library (http://sourceforge.net/projects/opencvlibrary/). The feature tracking is accomplished based on the technique introduced in (Georgescu and Meer, 2004). The resultant matching error between two consecutive frames is less than 1.0 pixel, with some outliers. Their average projection errors in 20 frames for each step are illustrated in Figure 3. It is clear that two-step iteration favors finding a desirable solution and bundle adjustment increases the stability and smoothness over a sequence. Figure 4 shows four representative key frames from each video sequence.

The sequence shown in the top row of Figure 4 demonstrates a case where the translation dominates the camera motion. The camera moves rightwards and rotates slightly. The scene contains a lot of intersections and occlusions which makes feature matching difficult. Traditional algorithms are hard to achieve precise solutions, especially for T. In contrast, our decomposition scheme favors highly accurate recovery of camera parameters as shown in Figure 3(a).

The second row of Figure 4 shows a scene where the camera moves backward slowly while rotates. The 2D movements are very small and thus camera estimation is very sensitive to the correspondence error. Fortunately, the 2D movements of each depth layer can be grouped correctly by our method, and facilitates both depth detection (Section 4.2) and initial camera estimation (Section 4.3). The average projection error shown in Figure 3(b) indicates the robustness of our method even under some occasional camera dithering.

The scene corresponding to the third row of Figure 4 is captured under a quite complex camera motion. The camera moves around and focuses on the far spot (shown in Red) all the time. Neither R nor T is dominant. Nevertheless, our method achieves relative low average projection error even without bundle adjustment as shown in Figure 3(c).

Among four video sequences, the scene shown in the last row of Figure 4 has the most complex camera motions. The camera motion exhibits a random-walk style. Figure 3(d) depicts the average projection error. Traditional methods result in relatively large projection errors due to high complexity and discontinuity of the camera motion. In our method, bundle adjustment is very useful for smoothing camera motion along a video sequence and making uniform structure, although the average projection error does not decrease greatly.

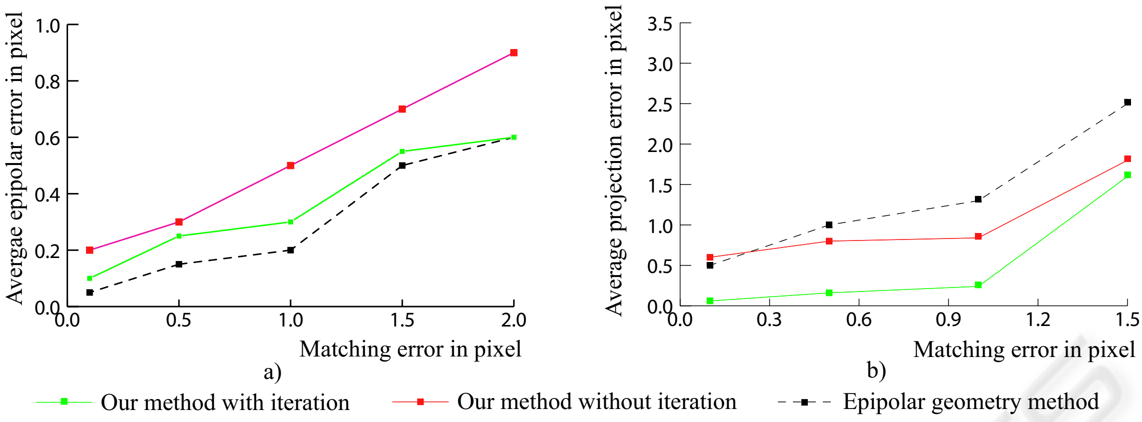

Figure 2: Comparisons of (a) epipolar errors and (b) projection errors among our method and traditional algorithms.

Our video submission encapsulates all four video sequences in which a sculpture is composed.

7 CONCLUSIONS AND FUTURE WORK

We have pursued a robust camera motion estimation method without any assumptions on the scene. The camera motion between two consecutive frames are decomposed into pure rotation and pure translation by inserting a virtual frame. Therefore, the 2D movements of feature points are separated into two parts owing to camera rotation and translation respectively. The initial evaluation of the rotation matrix is achieved by exploiting selected far feature points. The translation vector is then derived. Since the far feature points are not infinite far practically, the rotation matrix and translation vector need to be iteratively refined. Our experiments on both synthetic and real data demonstrate that our algorithm works well for general scenes, e.g., scenes containing extreme complicated, self-intersecting and inter-occluding objects.

Our future work includes improving the algorithm to work on sequences which include large area of moving object, moving objects detection and tracking, *etc*. In addition, dealing with an arbitrary-length video sequence is also in our schedule.

ACKNOWLEDGEMENTS

This paper is supported by NSF of China (Grant No.60373035), 973 program of China (No.2002CB312104), NSF of China for Innovative Research Groups (Grant No.60021201) and Specialized Research Fund for the Doctoral Program of Higher Education(No.20030335083).

REFERENCES

Alon, J. and Sclaroff, S. (2000). Recursive estimation of motion and planar structure. In *Proceedings of IEEE Computer Vision and Pattern Recognition*, pages 550–556.

Azarbayejani, A. and Pentland, A. P. (1995). Recursive estimation of motion, structure, and focal length. *IEEE Transactions on Pattern Analysis and Machine Intelligence*, 17(6):562–575.

Chen, Z., Pears, N., McDermid, J., and Heseltine, T. (2003). Epipolar estimation under pure camera translation. In *Proceedings of Digital Image Computing: Techniques and Applications 2003*, pages 849–858, Sydney, Australia.

Cornelis, K., Pollefeys, M., and Gool, L. V. (2001). Tracking based structure and motion recovery for augmented video productions.

Cornelis, K., Verbiest, F., and Gool, L. V. (2004). Drift detection and removal for sequential structure for motion algorithms. *IEEE Transactions on Pattern Analysis and Machine Intelligence*, 26(10):1249–1259.

Georgescu, B. and Meer, P. (2004). Point matching under large image deformations and illumination changes. *IEEE Transactions on Pattern Analysis and Machine Intelligence*, 26(6):647–688.

Hartley, R. and Zisserman, A. (2000). *Multiple view geometry in computer vision*. Cambridge University Press.

Jepson, A. D. and Heeger, D. J. (1991). A fast subspace algorithm for recovering rigid motion. In *Proceedings of IEEE Workshop on Visual Motion*, pages 124–131.

Johansson, B. (1990). View synthesis and 3D reconstruction of piecewise planar scenes using intersection lines between the planes. In *Proceedings of International Conference on Pattern Recognition 1999*, pages 54–59.

Kahl, F. and Heyden, A. (2001). Euclidean reconstruction and auto-calibration from continuous motion. In *Proceedings of International Conference on Computer Vision 2001*, pages 572–577, Vancouver, Canada.

MacLean, W. J. (1999). Removal of translation bias when using subspace methods. In *Proceedings of International Conference on Computer Vision 1999*, pages 753–758.

Nistér, D. (2004). An efficient solution to the five-point relative pose problem. *IEEE Transactions on Pattern Analysis and Machine Intelligence*, 26(6):756–777.

Pollefeys, M., Gool, L. V., Vergauwen, M., Verbiest, F., Cornelis, K., Tops, J., and Koch, R. (2004). Visual modeling with a hand-held camera. *International Journal of Computer Vision*, 59(3):207–232.

Qin, X., Nakamae, E., and Tadamura, K. (2002). Automatically compositing still images and landscape video sequences. *IEEE Computer Graphics and Appliactions*, 22(1):68–78.

Sharp, G. C., Lee, S. W., and Wehe, D. K. (2004). Multiview registration of 3D scenes by minimizing error between coordinate frames. *IEEE Transactions on Pattern Analysis and Machine Intelligence*, 26(8):1037–1050.

Shashua, A. and Werman, M. (1995). Trilinearity of three perspective views and its associated tensor. In *Proceedings of International Conference on Computer Vision 1995*, pages 920–925.

Stein, G. P. and Shashua, A. (2000). Model-based brightness constraints: On direct estimation of structure and motion. *IEEE Transactions on Pattern Analysis and Machine Intelligence*, 22(9):992–1025.

Wang, W. and Tsui, H. T. (2000). An SVD decomposition of essential matrix with eight solutions for the relative positions of two perspective cameras. In *Proceedings of the International Conference on Pattern Recognition 2000*, pages 1362–1365, Barcelona, Spain.

Wong, K. H. and Chang, M. M. Y. (2004). 3D model reconstruction by constrained bundle adjustment. In *Proceedings of the 17th International Conference on Pattern Recognition*, pages 902–905.

Zhang, Z. (1998). Determining the epipolar geometry and its uncertainty: A review. *International Journal of Computer Vision*, 27(2):161–198.

Zhang, Z. and Loop, C. (2001). Estimating the fundamental matrix by transforming image points in projective space. *Computer Vision and Image Understanding*, 82(2):174–180.

Zivkovic, Z. and van der Heijden, F. (2002). Better features to track by estimating the tracking convergence region. In *Proceedings of IEEE International Conference on Pattern Recognition 2002*, pages 635–638.

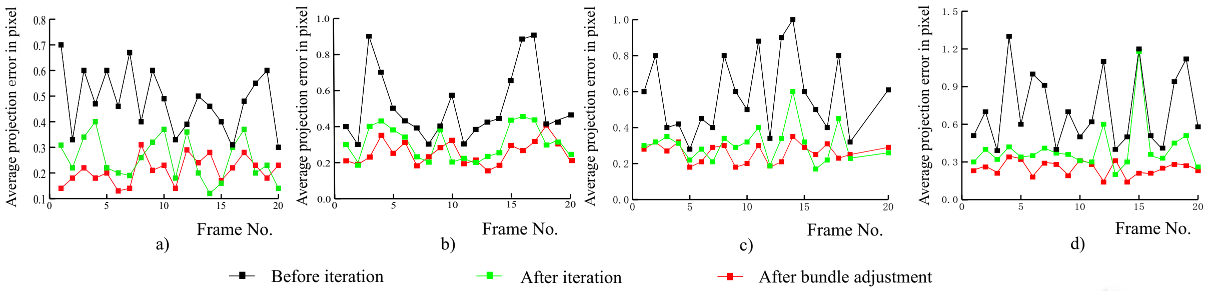

Figure 3: Average projection errors of four video sequences.

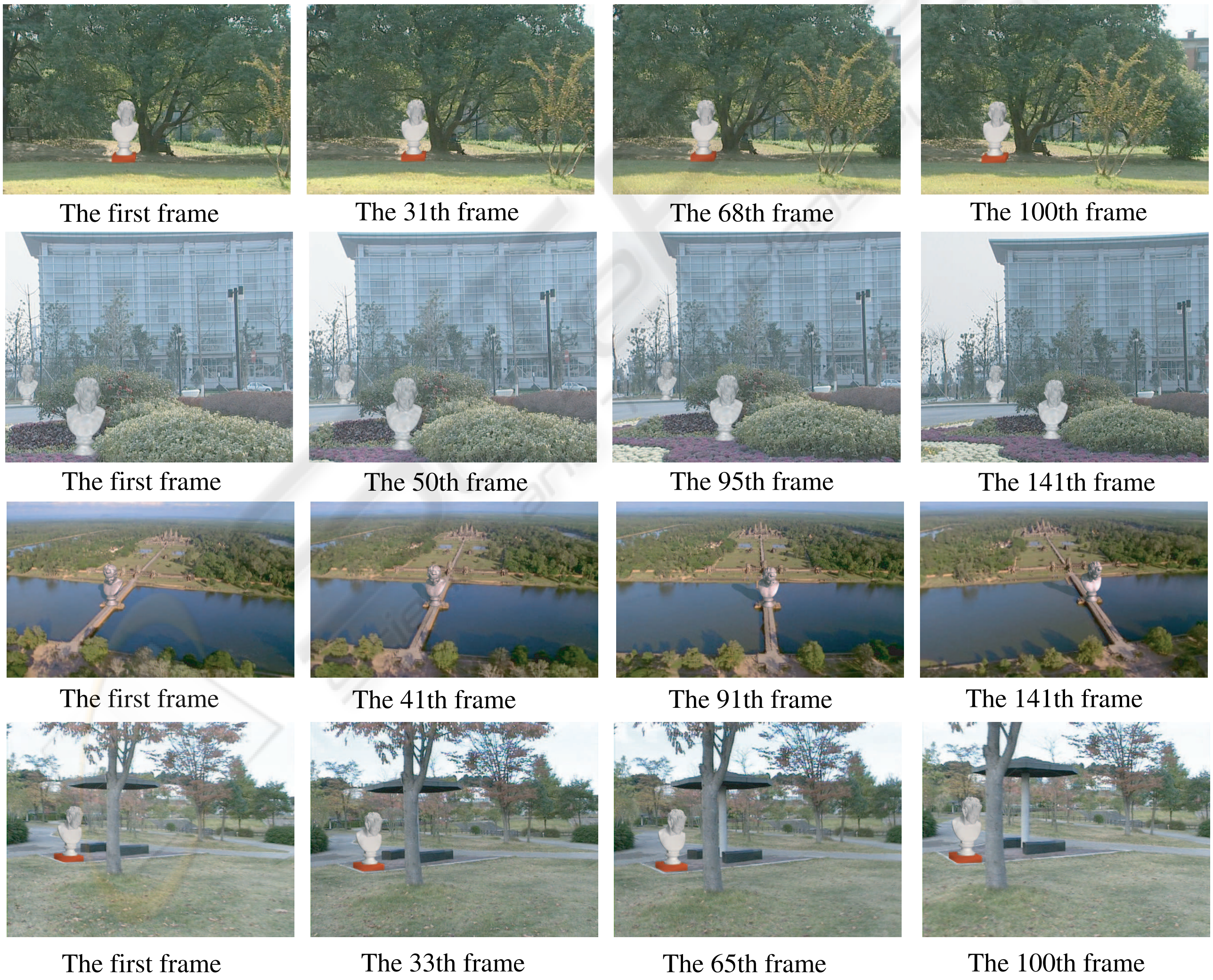
The first frame The 31th frame The 68th frame The 100th frame

The first frame The 50th frame The 95th frame The 141th frame

The first frame The 41th frame The 91th frame The 141th frame

The first frame The 33th frame The 65th frame The 100th frame

Figure 4: Key frames of four sequences where virtual objects are composed.